Epithelial Basement Membrane of Mouse Jejunum

Evidence for Laminin Turnover along the Entire Crypt–Villus Axis

Jerry S. Trier, Carol H. Allan, Dale R. Abrahamson,* and Susan J. Hagen

*Departments of Medicine, Brigham and Women's Hospital and Harvard Medical School and the Harvard Digestive Disease Center, Boston, Massachusetts 02115; and *Department of Cell Biology and Anatomy, University of Alabama at Birmingham, Birmingham, Alabama 35294*

Abstract

Little is known regarding turnover of the epithelial basement membrane in adult small intestine. Are components degraded and inserted along the length of the crypt–villus axis or selectively in the crypt region with subsequent migration of basement membrane from crypt to villus tip in concert with epithelium? We injected affinity-purified sheep anti–laminin IgG or sheep anti–laminin IgG complexed to horseradish peroxidase (HRP) into mice to label basement membrane laminin in vivo. Fluorescence microscopy revealed linear fluorescence along the length of the jejunal epithelial basement membrane 1 d after anti–laminin IgG injection. By 1 wk, small nonfluorescent domains were interposed between larger fluorescent domains. Over the next 5 wk the lengths of nonfluorescent domains increased progressively whereas those of fluorescent domains decreased. Additionally, electron microscopy revealed HRP reaction product along the length of the epithelial basement membrane after 1 d whereas unlabeled or lightly labeled domains that increased in length with time were observed interposed between heavily labeled domains by 2 and 4 wk along the entire crypt–villus axis. We conclude that laminin turnover occurs focally in the epithelial basement membrane of mouse jejunum along the crypt–villus axis over a period of weeks and that this basement membrane does not comigrate in concert with its overlying epithelium. (*J. Clin. Invest.* 1990. 86:87–95.) Key words: extracellular matrix • immunocytochemistry • immunofluorescence • morphometry • small intestine

Introduction

Polarized epithelia are intimately associated with extracellular matrix components that are organized into a basement membrane, which underlies their basal surface (1, 2). Epithelial basement membranes provide structural support for the epithelia to which they are applied. In addition, there is substantial evidence that interactions between epithelial cells and the extracellular matrix, particularly basement membrane components (*a*) promote cell adhesion to the extracellular matrix (3, 4), (*b*) induce expression of differentiated epithelial cell functions (5, 6), (*c*) initiate and maintain cell polarity (7, 8), (*d*) participate in the regulation of morphogenesis (9, 10), and (*e*) promote cell migration (11). In mature adult organs with limited cell proliferation, basement membranes are generally quite stable structures (12, 13). In tissues that proliferate actively during morphogenesis, in contrast, there is modification and more rapid turnover of basement membrane components (12, 13).

The basement membrane underlying the epithelium of the small intestine is a thin sheet 50–75 nm wide with scattered round and oval defects (14, 15). These gaps may be related to the trafficking of leukocytes, especially lymphocytes, between the lamina propria and the epithelial intercellular spaces and to the projection of pseudopod-like processes of epithelial cell basal cytoplasm into the lamina propria where they contact mesenchymal cells (14–16). The major components of the epithelial basement membrane of the small intestine, like that of other epithelial basement membranes, include type IV collagen, laminin, entactin/nidogen, and heparan sulfate proteoglycan in addition to the interstitial matrix components, fibronectin and type III procollagen (2, 17).

Unlike many epithelial organs in the adult, those of the tubular alimentary tract are characterized by rapid cell renewal of the epithelium. In the mammalian small intestine active epithelial cell proliferation is confined to crypts. Cells differentiate as they migrate out of the crypts and up the villi to the villus tips from which they exfoliate within 3–6 d after their formation in crypts (14). The small intestine would therefore appear to provide a useful model in which to examine in vivo the turnover of the components of a basement membrane applied to an epithelium composed of proliferating, differentiating, and mature cell populations.

In the small intestine, a sheath of pericryptal myofibroblasts is apposed to the abluminal surface of the basement membrane (18–20). Evidence for proliferation by pericryptal fibroblasts with their subsequent migration toward the villus tip led to the speculation that epithelium, basement membrane, and mesenchyme may normally migrate synchronously as a unit from crypt to villus tip (18). If true, progressive replacement of basement membrane from mid-crypt to villus tip would be expected in 3–6 d with each migration cycle. However, in other studies coordinated migration of fibroblasts and epithelium in small intestine could not be demonstrated (21, 22).

It has recently been shown that intravenous injection of polyclonal anti-laminin IgG into mice and rats labels basement membranes of organs with fenestrated capillaries, including those of the mucosa of the small intestine (23, 24). In the studies reported here, we labeled basement membrane of

This study was presented in part at the annual meeting of the American Gastroenterological Association, Washington, DC, 1989 May 14, and was published in abstract form (1989. *Gastroenterology.* 96:A515).

Address reprint requests to Dr. Trier, Gastroenterology Division, Brigham and Women's Hospital, 75 Francis Street, Boston, MA 02115.

Received for publication 16 November 1989 and in revised form 7 February 1990.

J. Clin. Invest.

0021-9738/90/08/0087/09 $2.00
Volume 86, July 1990, 87–95

the intestinal mucosa of mice in vivo with anti-laminin IgG and anti-laminin IgG coupled directly to horseradish peroxidase (HRP).[1] We used immunofluorescence and electron microscopy to assess the location of labeling and its subsequent decay along the crypt–villus axis and to determine whether or not the basement membrane migrates in concert with its overlying epithelium.

Methods

Animals. Male, adult BALB/c mice (Charles River Breeding Laboratories, Inc., Wilmington, MA) weighing 22–26 g were used in these studies.

Proteins and reagents. Laminin from murine Englebreth-Holm-Swarm tumor was purified (25, 26). The presence of other extracellular matrix components in this laminin preparation, including fibronectin, proteoglycans, or entactin/nidogen was not detected immunochemically (25), on polyacrylamide gels (24, 25, 27) or by rotary shadow electron microscopy (27). Anti-laminin IgG from previously immunized sheep was affinity-purified as described earlier (24, 25, 28) using laminin-Sepharose columns and was highly specific for laminin with no cross-reactivity with type IV collagen by an enzyme-labeled immunosorbent assay (28) or by Western blotting (data not shown). Sheep anti-laminin IgG and, for control studies, chromatographically pure sheep IgG (Organon Teknika-Cappel Laboratories, West Chester, PA) were conjugated directly (29) to activated HRP (type VI, Sigma Chemical Co., St. Louis, MO) as before (24, 25, 28). Rhodamine-conjugated rabbit anti-sheep IgG was obtained from Organon Teknika-Cappel Laboratories.

Administration of sheep anti-laminin IgG to mice. Mice were anesthetized by intraperitoneal injection of sodium pentobarbital (0.75–1 mg). The saphenous vein was exposed and 1 mg of anti-laminin IgG or control IgG in 0.3–0.5 ml of PBS (pH 7.4) was injected using a 30-gauge needle. Additional mice received 0.5 mg of anti-laminin IgG-HRP or, as controls, sheep IgG-HRP in 0.5 ml of PBS intravenously. The skin was sutured with silk and the mice were permitted to resume feeding upon awakening. Two mice were studied for each time point examined with each of the experimental IgG preparations.

Immunofluorescence microscopy. Mice were fasted overnight in metabolic cages but allowed access to water. Under sodium pentobarbital anesthesia the abdomen was opened via a midline incision and segments of proximal jejunum were removed 1, 7, 24, and 42 d after injection of anti-laminin IgG and 1 d after injection of control IgG. Unfixed pieces ~ 5 mm^2 were placed on cryostat chucks in OCT embedding medium (Miles Laboratories, Elkhart, IN) and frozen in isopentane cooled in liquid nitrogen. Cryostat sections, 4 μm thick, were mounted on poly-L-lysine-coated coverslips, air dried, and fixed for 5 min in acetone. After rehydration in PBS containing 0.02% gelatin, sections were incubated with rhodamine-conjugated rabbit anti-sheep IgG for 60 min at room temperature and mounted in glycerol containing *p*-phenylenediamine. Additional sections from mice killed 42 d after injection were preincubated with sheep anti-laminin IgG (150 μg/ml) before incubation with rhodamine-conjugated rabbit anti-sheep IgG. Sections were viewed and photographed with a Zeiss microscope (Carl Zeiss, Inc., Thornwood, NY) as described previously (30).

Immunoperoxidase microscopy. Segments of proximal jejunum from mice were removed as described above 1 d, 2 wk, and 4 wk after injection of sheep anti-laminin IgG-HRP and 1 d after injection of sheep control IgG-HRP, and quickly immersed in 2% paraformaldehyde and 2.5% gluteraldehyde buffered with 0.1 M cacodylate (pH 7.4) containing 0.01 M $CaCl_2$ for 2 h. After washing in cacodylate buffer, jejunal segments were embedded in 5% agar and cut into 50-μm sections parallel to the plane of the villi with a vibratome (EBTEC, Agawam, MA). Sections were washed in 0.1 M phosphate buffer (pH 6.0) with 3.5% sucrose, incubated at room temperature with 0.05% diaminobenzidine tetrachloride in 0.1 M phosphate buffer, pH 6.0 (31) for 30 min and then in the above medium containing 0.01% H_2O_2 (32) for 40 min. After washing in 0.1 M phosphate buffer (pH 7.4), sections were postfixed in 1% osmium tetroxide, and embedded in epoxy resin. Sections cut ~ 70 nm thick parallel to the plane of the villi were mounted on grids coated with formvar and carbon and viewed unstained or lightly stained with uranyl acetate and lead citrate with an electron microscope (model 300, Philips Electronic Instruments, Inc., Mahwah, NJ).

Morphometry. Micrographs of unstained sections of the mid-villus and crypt regions from mice injected with anti-laminin IgG-HRP were printed at a final magnification of 1,400 and coded. The percentage of epithelial basement membrane labeled with HRP was determined by measuring the length of the total basement membrane and the length of the portions that were discernibly labeled with HRP in each micrograph with a cursor using a Videoplan morphometry unit (Carl Zeiss, Inc.). The morphometric data from two mice for each time point were pooled and are presented as the means±SD. Means were compared by a one-way analysis of variance followed by the Neuman-Keuls multiple comparison test using a Statpac (Northwest Analytical, Inc., Portland, OR).

Results

Intravenous injection of anti-laminin IgG, anti-laminin IgG-HRP, or control IgGs did not alter jejunal mucosal structure, including that of the epithelial basement membrane, in recipient mice as assessed by light and electron microscopy. Moreover, injected mice did not develop diarrhea or lose weight but remained healthy throughout the duration of the experiments.

Localization of sheep anti-laminin IgG in jejunal mucosa by immunofluorescence microscopy. Representative immunofluorescence micrographs of frozen sections of jejunal villi and crypts from mice killed 1 d, 1 wk, and 6 wk after injection of anti-laminin IgG are shown in Figs. 1 and 2 after incubation with rhodamine-conjugated rabbit anti-sheep IgG. Fluorescence along the length of the villus and crypt epithelial basement membrane was virtually continuous 1 d after injection (Figs. 1 *a* and 2 *a*), indicating that laminin was present in mouse intestine throughout the epithelial basement membrane from crypt base to villus tip. Linear fluorescence along the basement membranes of mucosal capillaries, nerves, and smooth muscle was also seen (Figs. 1 *a* and 2 *a*). In contrast, sections from mice injected with control sheep IgG 1 d earlier and then incubated with rhodamine-conjugated rabbit anti-sheep IgG showed no fluorescence along the mucosal basement membranes (data not shown). 1 wk after injection of anti-laminin, epithelial basement membrane fluorescence assumed a speckled pattern consisting of small domains with little or no fluorescence that were interposed between domains that remained strongly fluorescent (Figs. 1 *b* and 2 *b*). By 24 d and 6 wk after injection of anti-laminin IgG, the lengths of the lightly fluorescent and nonfluorescent domains increased with a concomitant decrease in the lengths of domains with strong fluorescence (Figs. 1 *c* and 2 *c*). This indicates that bound anti-laminin IgG was gradually depleted from discrete domains of the epithelial basement membrane along the length of the crypt–villus axis.

Preincubation of frozen sections of jejunum, obtained from mice 6 wk after anti-laminin IgG injection, with sheep anti-laminin IgG before incubation with rhodamine-conjugated rabbit anti-sheep IgG resulted in intense, continuous

1. *Abbreviation used in this paper:* HRP, horseradish peroxidase.

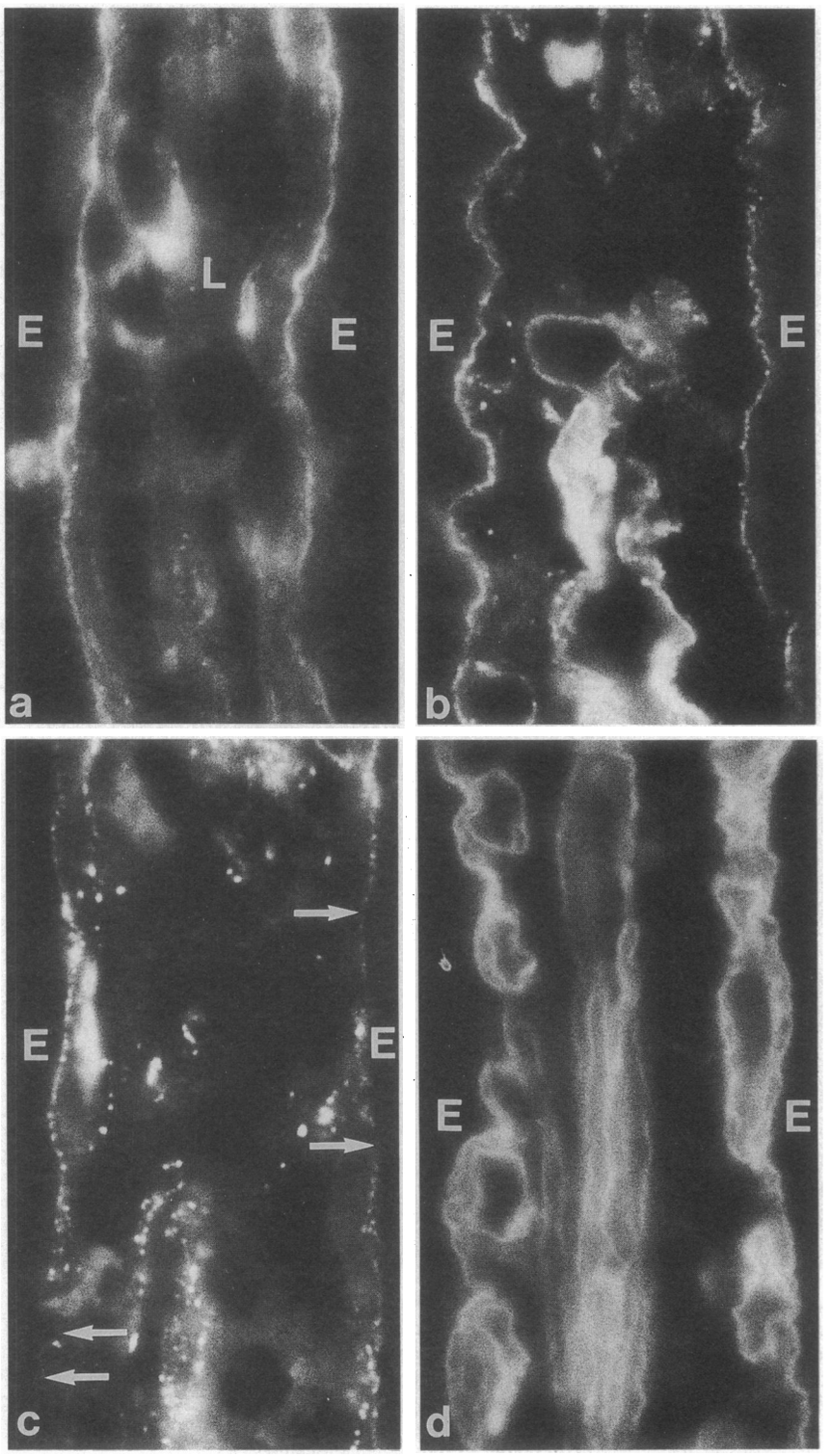

Figure 1. Fluorescent antibody staining of frozen sections of mouse jejunal villi. (*a*) 1 d after injection of sheep anti–laminin IgG followed by in vitro exposure to rhodamine-conjugated rabbit anti–sheep IgG, there is linear fluorescence of the basement membrane underlying the epithelium (*E*). Fluorescence in the lamina propria (*L*) in this micrograph and in *b*, *c*, and *d* represents capillary, nerve, and muscle basement membrane. ×1,800. (*b*) 1 wk after injection of sheep anti–laminin IgG followed by in vitro exposure to rhodamine-conjugated rabbit anti–sheep IgG, the fluorescence of the basement membrane underlying the epithelium (*E*) has a speckled appearance. ×1,800. (*c*) 6 wk after injection of sheep anti–laminin IgG followed by in vitro exposure to rhodamine-conjugated rabbit anti-sheep IgG, the segments of basement membrane underlying epithelium (*E*) with intense fluorescence have decreased in length whereas segments with no or faint fluorescence (*arrows*) have increased in length. ×1,800. (*d*) Adjacent section from the villus shown in *c* preincubated in sheep anti–laminin in vitro before exposure to rhodamine-conjugated rabbit anti–sheep IgG. There is linear fluorescence of the basement membrane underlying the epithelium (*E*). ×1,800. Photographic exposure for *a*, *b*, and *c* was 15 s whereas exposure for *d* was 4 s.

linear fluorescence of the epithelial basement membrane along the entire length of the crypt–villus axis (Figs. 1 *d* and 2 *d*). This observation suggests that the nonfluorescent domains of epithelial basement membrane observed 7 d or more after injection of anti–laminin antibody contained newly synthesized laminin that was incorporated into the basement membrane during the interval between anti–laminin IgG injection and sacrifice of the mouse.

Localization of sheep anti–laminin IgG-HRP in jejunal mucosa by electron microscopy. 1 d after injection of anti–laminin IgG-HRP, electron-dense peroxidase reaction product decorated the epithelial basement membrane at the interface of epithelium and the lamina propria along the length of the jejunal villi (Fig. 3 *a*) and along most of the laminin propria–epithelial interface along jejunal crypts (Fig. 4 *a*). Gaps in basement membrane labeling were consistently observed,

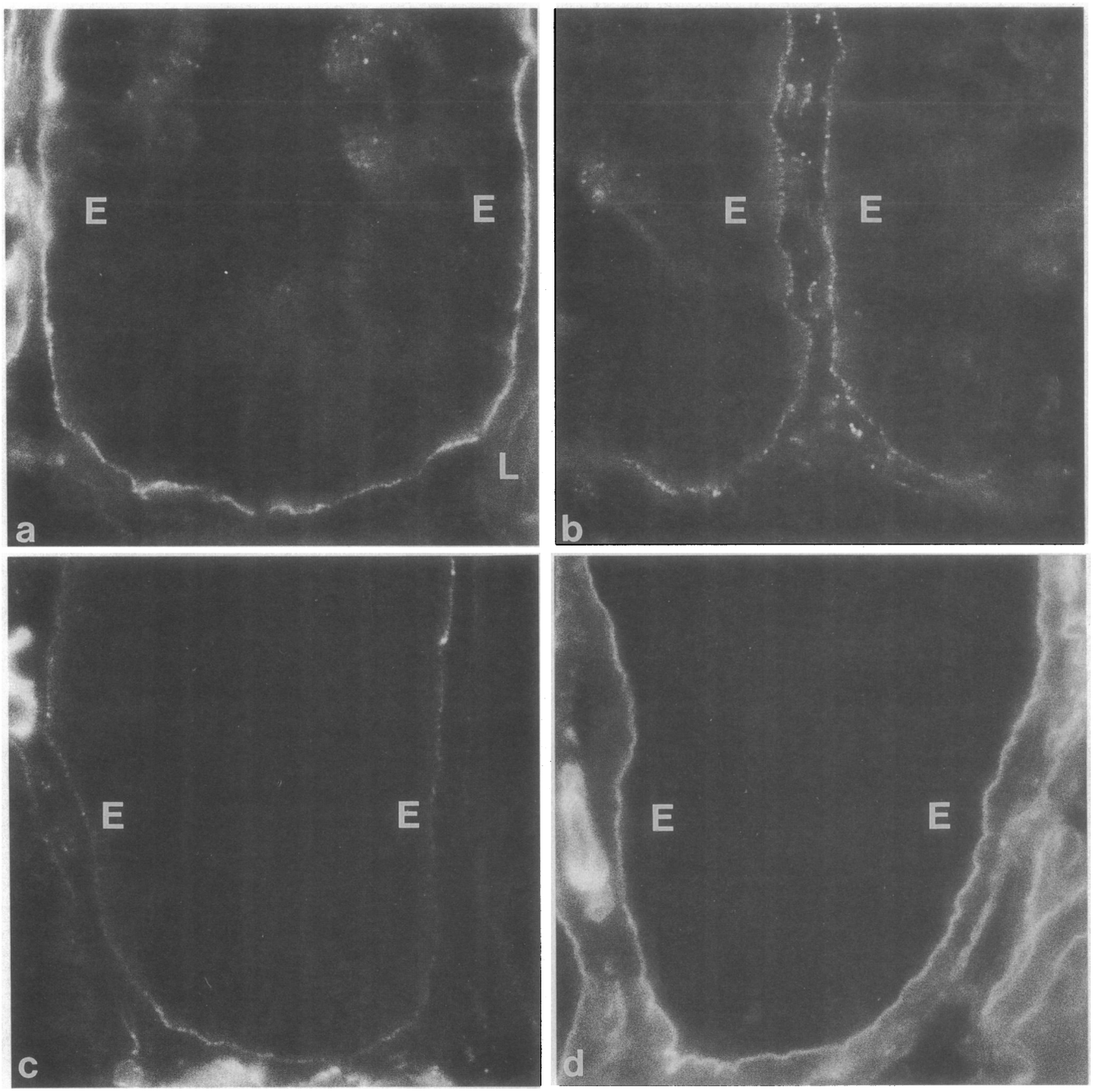

Figure 2. Fluorescent antibody staining of frozen sections of mouse jejunal crypts. The experimental procedure for *a, b, c,* and *d* correspond to *a, b, c,* and *d* in Fig. 1. (*a*) 1 d after injection of sheep anti–laminin IgG, basement membrane fluorescence underlying epithelium (*E*) is essentially linear with few gaps. Fluorescence in the lamina propria (*L*) in this micrograph and in *b, c,* and *d* represents capillary, nerve, and muscle basement membrane. ×1,800. (*b*) 1 wk after injection of sheep anti–laminin IgG, basement membrane fluorescence underlying epithelium (*E*) has a speckled pattern. ×1,800. (*c*) 6 wk after injection of sheep anti–laminin IgG, segments of basement membrane with faint or no fluorescence underlying epithelium (*E*) have increased in length. ×1,800. (*d*) After preincubation in sheep anti–laminin, in vitro fluorescence of a section adjacent to that shown in *c* demonstrates linear fluorescence of the basement membrane underlying epithelium (*E*). ×1,800.

however, at sites where there was migration of lamina propria cells into the intercellular spaces between epithelial cells (Fig. 5). Gaps in labeling were also seen where processes of epithelial cell cytoplasm projected into the lamina propria as well as in occasional focal areas within intact basement membrane, especially along crypts. Capillary, nerve, and smooth muscle basement membranes in the lamina propria were usually decorated linearly along their length with electron-dense reaction product. In contrast, in mice killed 1 d after injection with control sheep IgG-HRP, reaction product was apparent only in structures with endogenous peroxidase activity (such as peroxisomes) but not along basement membranes.

2 wk after injection of anti–laminin IgG-HRP, focal lengths of basement membrane that were heavily decorated

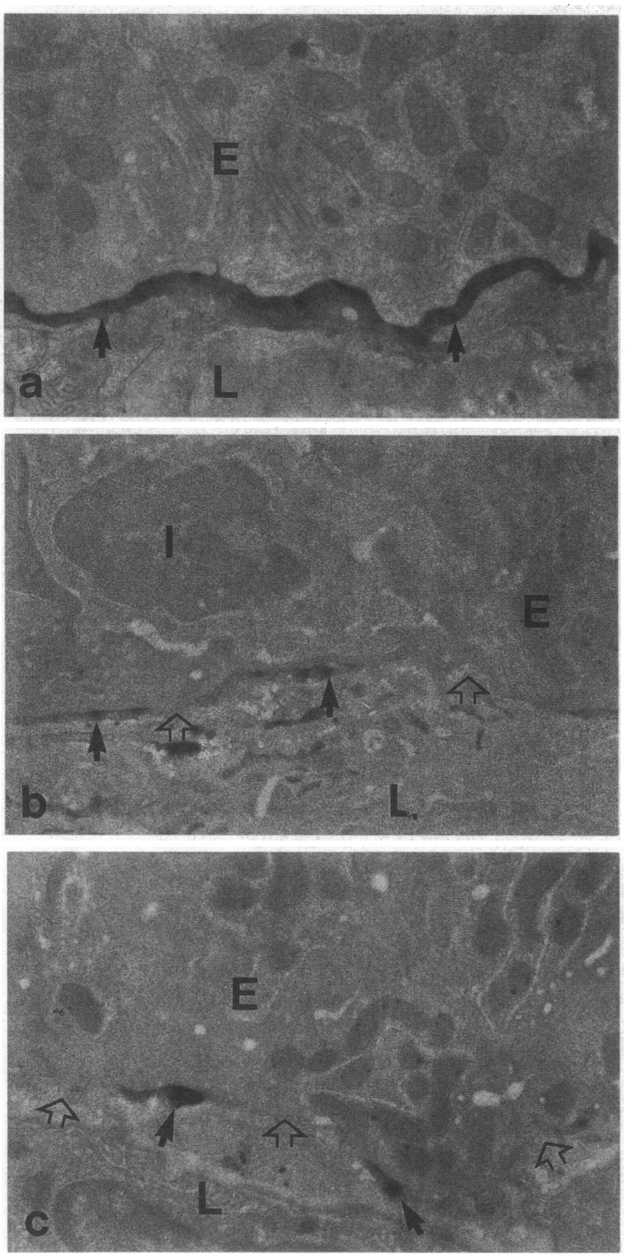

Figure 3. Electron micrographs of unstained sections at the interface of epithelium and lamina propria from the midvillus region of jejunum from mice that had received sheep anti–laminin IgG-HRP intravenously. (*a*) 1 d after injection of anti–laminin IgG-HRP, there is HRP-reaction product along the length of the epithelial basement membrane (*solid arrows*). *E,* epithelium; *L,* lamina propria. ×10,400. (*b*) 2 wk after injection of anti–laminin IgG-HRP, segments of epithelial basement membrane without HRP-reaction product (*open arrows*) are interposed between segments with reaction product (*solid arrows*). *E,* epithelium; *I,* intraepithelial lymphocyte; *L,* lamina propria. ×10,400. (*c*) 4 wk after injection of anti–laminin IgG-HRP, the segments of epithelial basement membrane with no HRP-reaction product have increased in length (*open arrows*) whereas those with reaction product (*solid arrows*) have decreased in length. *E,* epithelium; *L,* lamina propria. ×10,400.

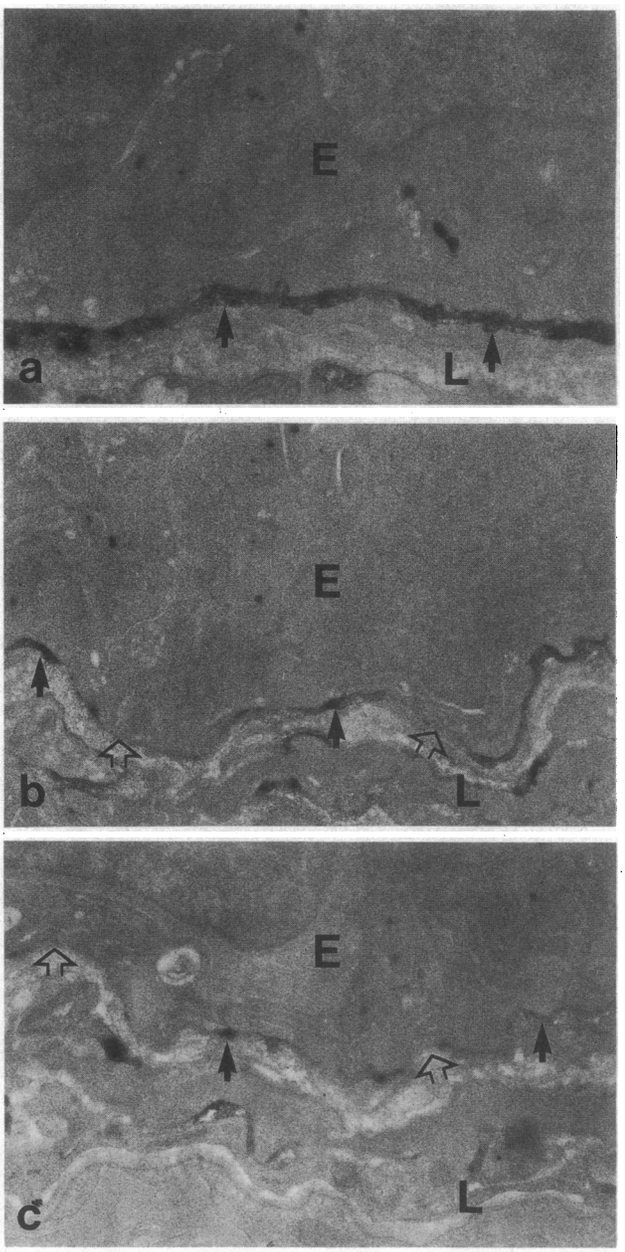

Figure 4. Electron micrographs of unstained sections of the interface at epithelium and lamina propria from the crypt region of jejunum from mice that had received sheep anti–laminin IgG-HRP intravenously. (*a*) 1 d after injection of anti–laminin IgG-HRP, there is decoration with HRP-reaction product along the length of the epithelial basement membrane (*solid arrows*). *E,* epithelium; *L,* lamina propria. ×10,400. (*b*) 2 wk after injection of anti–laminin IgG-HRP, segments of epithelial basement membrane without HRP-reaction product (*open arrows*) are interposed between segments with reaction product (*solid arrows*). *E,* epithelium; *L,* lamina propria. ×10,400. (*c*) 4 wk after injection of anti–laminin IgG-HRP, the segments of epithelial basement membrane with faint or no reaction product are longer (*open arrows*) whereas those with intense reaction product are shorter (*solid arrows*) than were observed at 2 wk. *E,* epithelium; *L,* lamina propria. ×10,400.

with reaction product were interrupted by weakly decorated or unlabeled lengths along villus epithelium (Fig. 3 *b*) and along crypt epithelium (Fig. 4 *b*). By 4 wk the domains of epithelial basement membrane with peroxidase activity were smaller and those without activity were larger than was noted at 2 wk both in villi (Fig. 3 *c*) and in crypts (Fig. 4 *c*). In contrast, the

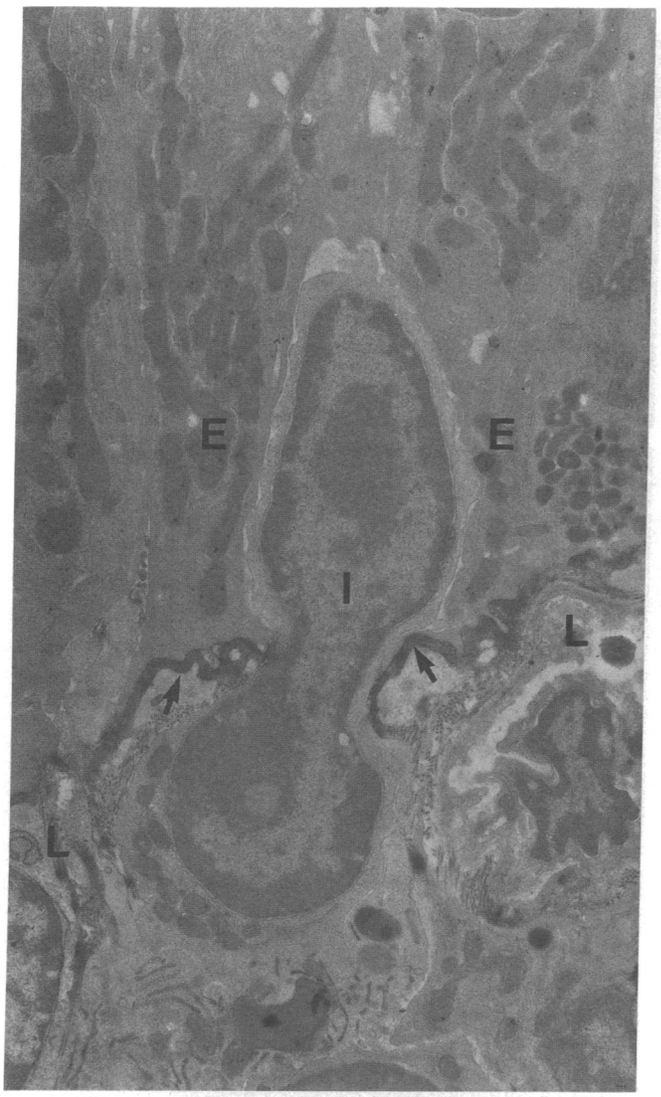

Figure 5. Electron micrograph of the epithelial–mesenchymal interface of a jejunal villus from a mouse that had received sheep anti–laminin IgG-HRP intravenously 1 d earlier. There is a gap in the epithelial basement membrane where a lymphocyte (*I*) is traversing the interface between the epithelium (*E*) and the lamina propria (*L*). On each side of the gap the basement membrane is decorated with HRP-reaction product (*arrows*). Lightly stained with uranyl acetate and lead citrate. ×8,300.

basement membrane associated with most nerve fibers and smooth muscle cells but not capillaries remained intensely decorated with reaction product 4 wk after anti–laminin IgG-HRP injection, even when located proximate to sparsely labeled epithelial basement membrane (Fig. 6).

Morphometry. Morphometric assessment of labeling of the villus and crypt epithelial basement membrane 1 d, 2 wk, and 4 wk after administration of anti–laminin IgG-HRP is summarized in Fig. 7. The extent of labeling of villus basement membrane decreased from 95% at 1 d to 54% at 2 wk, and to 26% at 4 wk. All three mean values differed from one another ($P < 0.01$) despite considerable variation among some pairs. Similarly, labeling of crypt basement membranes decreased from 86% at one day to 35% at 2 wk and to 11% at 4 wk. Again, all three mean values differed from one another ($P < 0.01$).

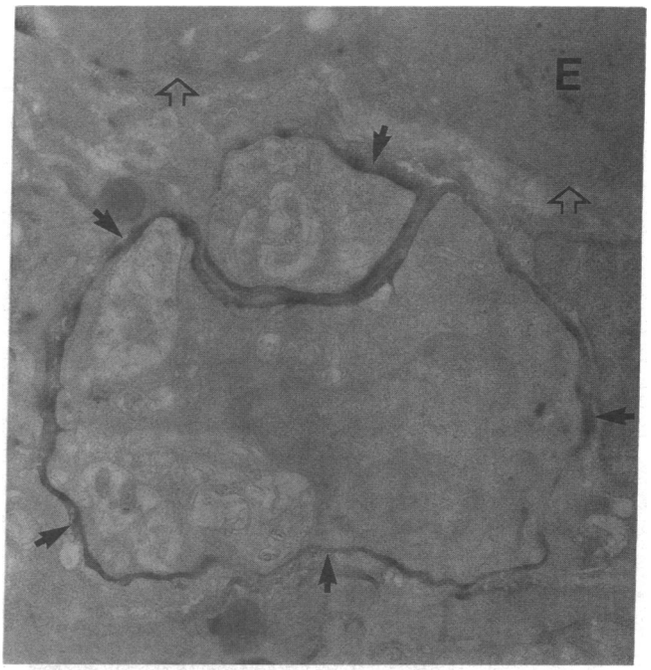

Figure 6. Unstained electron micrograph of nerve fibers in lamina propria that are in close proximity to epithelium (*E*) from a mouse that had received sheep anti–laminin IgG-HRP intravenously 4 wk earlier. The basement membranes enclosing nerve fibers are decorated along most of their length (*solid arrows*) with HRP-reaction product whereas the adjacent epithelial basement membrane (*open arrows*) is largely devoid of reaction product. ×12,100.

Discussion

These studies, in which laminin was labeled in vivo with anti–laminin IgG, demonstrate that laminin is present throughout the basement membrane that underlies the jejunal epithelium of adult mice from crypt base to villus tip, confirming earlier observations in mice and other mammalian species (17, 24, 33). Moreover, the persistence of some anti–laminin IgG along the length of the crypt–villus axis for as long as 6 wk provides strong evidence that the basement membrane does not comi-

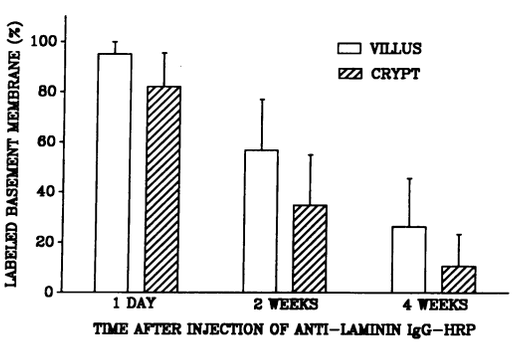

Figure 7. Percentage of jejunal villus and crypt epithelial basement membrane decorated with HRP-reaction product as determined by morphometric measurements from mice killed 1 d, 2 wk, and 4 wk after intravenous injection of sheep anti–laminin IgG-HRP. Each bar shows the mean and SD of measurements from 10 micrographs from each of two mice for the villus basement membrane and the mean and SD of measurements from five micrographs from each of two mice for the crypt basement membrane.

grate with its overlying epithelium or underlying myofibroblasts. Mouse jejunal epithelial cells migrate from their origin in the crypts to the extrusion zone on the tips of villi in 48–72 h (21). Therefore, if comigration of basement membrane and epithelium had occurred, loss of basement membrane labeling in the upper crypt region and base of villi by 1 d and virtual disappearance of basement membrane labeling by 1 wk after anti-laminin IgG injection should have been observed. Instead, our findings indicate that the intestinal epithelial basement membrane appears to be a relatively stable structure that provides a scaffold on which epithelial cells and perhaps subepithelial myofibroblasts migrate. Additional evidence for migration of intestinal epithelial cells along their underlying basement membrane is found in recent studies in which viable epithelial cells rapidly covered denuded basement membrane after destruction of the epithelium on the upper portion of villi (34, 35).

Basement membranes in most tissues of adult animals appear to be remarkably stable structures with a long half-life and slow turnover of their components (13, 36). However, the epithelial basement membrane of the small intestine and other tubular digestive organs are unusual among those of adult tissues in that they support and interact with cell populations undergoing rapid renewal (14, 37). Hence, substantial turnover of basement membrane components might be expected since there is rapid basement membrane assembly in actively growing fetal and neonatal tissues (13, 38) and rapid basement membrane degradation accompanies involution of the post partum mammary gland (39). Although our studies indicate that the overall turnover of the jejunal epithelial basement membrane is slow, they suggest that constant remodeling of the epithelial basement membrane of adult mouse jejunum takes place. When anti-laminin IgG was injected intravenously, the antibodies initially labeled in a linear fashion virtually the entire epithelial basement membrane as assessed by fluorescence and electron microscopy. Subsequently, IgG labeling of the basement membrane decreased progressively with the passage of time along the entire crypt–villus axis but the intensity of labeling did not decrease uniformly. Rather, strongly labeled domains were interposed between unlabeled and lightly labeled domains for up to 4 and 6 wk after injection of anti-laminin IgG-HRP (Figs. 3 *c* and 4 *c*) and anti-laminin IgG (Figs. 1 *c* and 2 *c*), respectively. However, that the unlabeled domains contained abundant laminin was shown by in vitro exposure of these tissues to anti-laminin IgG (Figs. 3 *d* and 4 *d*). This pattern of fluorescence decay with time in the epithelial basement membrane of adult mouse jejunum differed strikingly from that observed in glomerular basement membrane of adult rat kidney in which fluorescence remained linear for at least 10 wk after anti-laminin IgG injection (25). On the other hand, the appearance with time of alternating labeled and unlabeled segments along the epithelial basement membrane of the adult mouse jejunum is remarkably similar to that observed in glomerular, adrenal, and pituitary basement membranes of newborn rats after injection of anti-laminin IgG (13, 28, 38). In those studies, reexposure to anti-laminin IgG in vivo at later times resulted in decoration of the unlabeled basement membrane segments with the antibody leading to the interpretation that newly synthesized matrix is progressively spliced into old in these rapidly growing tissues (12, 28, 38). A similar process may occur during epithelial basement membrane renewal in the jejunum of adult mice.

There are several factors that may contribute to the turnover of laminin (and perhaps other matrix components) in the epithelial basement membrane of the mouse intestine. First, local protease production by epithelial or lamina propria cells may regulate, by proteolysis of laminin and other matrix components (40), detachment and reattachment of the epithelial cell basal membrane to the basement membrane during crypt to villus migration. If this occurs, however, the laminin in some basement membrane domains appears to be more susceptible to digestion than in others. Secondly, the movement of leukocytes across the basement membrane as they migrate between the lamina propria and epithelial cell intercellular spaces may have contributed to the discontinuous pattern of basement membrane labeling observed several weeks after anti-laminin IgG injection. Such trafficking of cells from lamina propria to epithelium is a dynamic process (41, 42) and occurs through discontinuities in the basement membrane (Fig. 5). It seems possible that such gaps are produced by the migrating cells at the point of basement membrane penetration and are then rapidly sealed by the reassembly of matrix components, since basement membrane defects are not usually observed underlying intraepithelial lymphocytes not in the process of traversing the basement membrane. Thirdly, the formation of pseudopod-like processes of epithelial basal cytoplasm that extend into the underlying mesenchyme through gaps in the basement membrane (14, 16) may have contributed to focal basement membrane degradation and its subsequent reassembly. Fourthly, some nonspecific dissociation of bound anti-laminin IgG from its binding sites may have occurred. If so, the turnover of laminin in the epithelial basement membrane of adult mouse jejunum would be even slower than our results indicate. However, the focal loss of anti-laminin IgG from some basement membrane domains and its retention in adjacent domains cannot be readily explained by nonspecific dissociation alone. Additionally, the persistence of anti-laminin IgG tracer in basement membranes of nerve fibers juxtaposed to unlabeled epithelial basement membrane (Fig. 6) suggests that mechanisms other than nonspecific dissociation of anti-laminin IgG from laminin contributed to the loss with time of label from the epithelial basement membrane.

Studies in which explants of intestinal endoderm or mesenchyme from fetal rats or mice were cultured separately or while in direct contact with one another suggest that the presence of both mesenchyme and epithelium is essential for basement membrane formation and epithelial cell differentiation (43–45). By the use of species specific antibodies and interspecies grafts of rat and chick fetal intestinal mesenchyme and endoderm, it has recently been shown that type IV collagen is produced by mesenchymal cells and heparan sulfate proteoglycan is produced by the epithelium in the basement membrane that forms at the epithelial–mesenchymal interface of these grafts (45, 46). In another recent study, expression of laminin mRNA has been detected by in situ hybridization in the lamina propria but not in epithelium of the small intestine of mouse fetuses (47). Less is known regarding the site of production of specific basement membrane components in the intestine of adult animals. Expression of laminin mRNA was not detected by in situ hybridization in adult mouse intestine (47) but a preliminary report detected in dot blot preparations type IV collagen α-chain mRNA in the lamina propria and laminin B-chain mRNA in the lamina propria and crypt epi-

thelium of small intestine from adult rats (48). Our studies do not provide information on the cellular origin of new laminin in adult intestine but disappearance of bound anti-laminin IgG took place in epithelial basement membrane along the entire crypt–villus axis. This suggests that considerable degradation and assembly of basement membrane underlying both the undifferentiated, differentiating, and differentiated compartments of the epithelium occur in the small intestine of adult mice. Since studies in the small intestine of the adult rat suggest that other basement membrane components, including entactin/nidogen, type IV collagen, and heparan sulfate proteoglycan, like laminin, are distributed uniformly along the crypt–villus axis in the epithelial basement membrane (17), study of the in vivo turnover of these molecules in intestinal mucosa should also be of interest.

In summary, the major findings of this study are (*a*) laminin turnover occurs focally in the epithelial basement membrane of mouse jejunum along the entire crypt–villus axis over a period of weeks, and (*b*) the jejunal epithelial basement membrane does not comigrate in concert with its overlying epithelium since the villus epithelium, unlike its basement membrane, is replaced in 2–3 d.

Acknowledgments

This work was supported by National Institutes of Health grants DK-36835, DK-34972, and DK-34854. Dr. Abrahamson is an Established Investigator of the American Heart Association.

References

1. Timpl, R., and G. R. Martin. 1982. Components of basement membranes. *In* Immunochemistry of the Extracellular Matrix. H. Furthmayr, editor. CRC Press, Inc., Boca Raton, FL. 119–150.

2. Laurie, G. W., C. P. Leblond, and G. R. Martin. 1982. Localization of type IV collagen, laminin, heparan sulfate proteoglycan, and fibronectin to the basal lamina of basement membranes. *J. Cell Biol.* 95:340–344.

3. Terranova, V. P., C. N. Rao, I. M. Margulies, and L. A. Liotta. 1983. Laminin receptor on human breast carcinoma cells. *Proc. Natl. Acad. Sci. USA.* 80:444–448.

4. Graf, J., Y. Iwamoto, M. Sasaki, G. R. Martin, H. K. Kleinman, F. A. Robey, and Y. Yamada. 1987. Identification of an amino acid sequence in laminin mediating cell attachment, chemotaxis, and receptor binding. *Cell.* 48:989–996.

5. Hadley, M. A., S. W. Byers, C. A. Suarez-Quian, H. K. Kleinman, and M. Dym. 1985. Extracellular matrix regulates Sertoli cell differentiation, testicular cord formation, and germ cell development in vitro. *J. Cell Biol.* 101:1511–1522.

6. Bissel, D. M., D. M. Arenson, J. J. Maher, and F. J. Roll. 1987. Support of cultured hepatocytes by a laminin-rich gel: evidence for a functionally significant subendothelial matrix in normal rat liver. *J. Clin. Invest.* 79:801–812.

7. Ingber, D. E., J. A. Madri, and J. D. Jamieson. 1986. Basement membrane as a spatial organizer of polarized epithelia: exogenous basement membrane reorients pancreatic epithelial tumor cells in vitro. *Am. J. Pathol.* 122:129–139.

8. Vega-Salas, D. E., P. J. I. Salas, D. Gundersen, and E. Rodriguez-Boulan. 1987. Formation of the apical pole of epithelial (Madin-Darby canine kidney) cells: polarity of an apical protein is independent of tight junctions while segregation of a basolateral marker requires cell-cell interactions. *J. Cell Biol.* 104:905–916.

9. Bernfield, M., and S. D. Banerjee. 1982. The turnover of basal lamina glycosaminoglycan correlates with epithelial morphogenesis. *Dev. Biol.* 90:291–305.

10. Hay, E. D. 1984. Cell-matrix interaction in the embryo: cell shape, cell surface, cell skeletons, and their role in differentiation. *In* The Role of Extracellular Matrix in Development. R. L. Trelstad, editor. Alan R. Liss, Inc., New York. 1–31.

11. Goodman, S. L., G. Risse, and K. von der Mark. 1989. The E8 subfragment of laminin promotes locomotion of myoblasts over extracellular matrix. *J. Cell Biol.* 109:799–809.

12. Bernfield, M., S. D. Banerjee, J. E. Koda, and A. C. Rapraeger. 1984. Remodelling of the basement membrane: morphogenesis and maturation. *In* Basement Membranes and Cell Movement. *Ciba Found. Symp.* 108:179–196.

13. Leardkamolkarn, V., and D. R. Abrahamson. 1988. Binding of intravenously injected antibodies against laminin to developing and mature endocrine glands. *Cell Tissue Res.* 251:171–181.

14. Madara, J. L., and J. S. Trier. 1987. Functional morphology of the mucosa of the small intestine. *In* Physiology of the Gastrointestinal Tract. L. R. Johnson, editor. Raven Press, New York. 1209–1249.

15. McClugage, S. G., and F. N. Low. 1984. Microdissection by ultrasonication: porosity of the intestinal epithelial basal lamina. *Am. J. Anat.* 171:207–216.

16. Mathan, M., J. A. Hermos, and J. S. Trier. 1972. Structural features of the epithelio-mesenchymal interface of rat duodenal mucosa during development. *J. Cell Biol.* 52:577–588.

17. Simon-Assmann, P., M. Kedinger, and K. Haffen. 1986. Immunocytochemical localization of extracellular-matrix proteins in relation to rat intestinal morphogenesis. *Differentiation.* 32:59–66.

18. Parker, F. G., E. N. Barnes, and G. I. Kaye. 1974. The pericryptal fibroblast sheath. VI. Replication, migration, and differentiation of the subepithelial fibroblasts of the crypt and villus of the rabbit jejunum. *Gastroenterology.* 67:607–621.

19. Marsh, M. N., and J. S. Trier. 1974. Morphology and cell proliferation of subepithelial fibroblasts in adult mouse jejunum. I. Structural features. *Gastroenterology.* 67:622–635.

20. Joyce, N. C., M. F. Haire, and G. E. Palade. 1987. Morphologic and biochemical evidence for a contractile cell network within the rat intestinal mucosa. *Gastroenterology.* 92:68–81.

21. Marsh, M. N., and J. S. Trier. 1974. Morphology and cell proliferation of subepithelial fibroblasts in adult mouse jejunum. II. Radioautographic studies. *Gastroenterology.* 67:636–645.

22. Neal, J. V., and C. S. Potten. 1981. Description and basic cell kinetics of the murine pericryptal fibroblast sheath. *Gut.* 22:19–24.

23. Yaar, M., J. M. Foidart, K. S. Brown, S. I. Rennard, G. R. Martin, and L. Liotta. 1982. The Goodpasture-like syndrome in mice induced by intravenous injections of anti-type IV collagen and anti-laminin antibody. *Am. J. Pathol.* 107:079–091.

24. Abrahamson, D. R., and J. P. Caulfield. 1985. Distribution of laminin within rat and mouse renal, splenic, intestinal, and hepatic basement membranes identified after the intravenous injection of heterologous antilaminin IgG. *Lab Invest.* 52:169–181.

25. Abrahamson, D. R., and J. P. Caulfield. 1982. Proteinuria and structural alterations in rat glomerular basement membranes induced by intravenously injected anti-laminin immunoglobulin G. *J. Exp. Med.* 156:128–145.

26. Timpl, R., H. Rohde, P. G. Robey, S. I. Rennard, J. M. Foidart, and G. R. Martin. 1979. Laminin—a glycoprotein from basement membranes. *J. Biol. Chem.* 254:9933–9937.

27. Abrahamson, D. R., M. H. Irwin, P. L. St. John, E. W. Perry, M. A. Accavitti, L. Heck, and J. R. Couchman. 1989. Selective immunoreactivities of kidney basement membranes to monoclonal antibodies against laminin: localization of the end of the long and short arms to discrete microdomains. *J. Cell Biol.* 109:3477–3491.

28. Abrahamson, D. R. 1985. Origin of the glomerular basement membrane visualized after in vivo labeling of laminin in newborn rat kidneys. *J. Cell Biol.* 100:1988–2000.

29. Nakane, P. K., and A. Kawaoi. 1974. Peroxidase-labeled antibody: a new method of conjugation. *J. Histochem. Cytochem.* 22:1084–1091.

30. Hagen, S. J., and J. S. Trier. 1988. Immunocytochemical local-

ization of actin in epithelial cells of rat small intestine by light and electron microscopy. *J. Histochem. Cytochem.* 36:717–727.

31. Rodewald, R. 1980. Distribution of immunoglobulin G receptors in the small intestine of the young rat. *J. Cell Biol.* 85:18–32.

32. Graham, R. C., and M. J. Karnovsky. 1966. The early stages of absorption of injected horseradish peroxidase in the proximal tubules of mouse kidney: ultrastructural cytochemistry by a new technique. *J. Histochem. Cytochem.* 14:291–302.

33. Martinez-Hernandez, A., and A. E. Chung. 1984. The ultrastructural localization of two basement membrane components: entactin and laminin in rat tissues. *J. Histochem. Cytochem.* 32:289–298.

34. Feil, W., E. Wenzl, P. Vattay, M. Starlinger, T. Sogukoglu, and R. Schiessel. 1987. Repair of rabbit duodenal mucosa after acid injury in vivo and in vitro. *Gastroenterology.* 92:1973–1986.

35. Moore, R., S. Carlson, and J. L. Madara. 1989. Rapid barrier restitution in an *in vitro* model of intestinal epithelial injury. *Lab. Invest.* 60:237–244.

36. Price, R. G., and R. G. Spiro. 1977. Studies on the metabolism of the renal glomerular basement membrane: turnover measurements in the rat with the use of radiolabeled amino acids. *J. Biol. Chem.* 252:8597–8602.

37. Eastwood, G. L. 1977. Gastrointestinal epithelial renewal. *Gastroenterology.* 72:962–975.

38. Abrahamson, D. R., and E. W. Perry. 1986. Evidence for splicing new basement membrane into old during glomerular development in newborn rat kidneys. *J. Cell Biol.* 103:2489–2498.

39. Martinez-Hernandez, A., L. M. Fink, and G. B. Pierce. 1976. Removal of basement membrane in the involuting breast. *Lab. Invest.* 34:455–462.

40. McGuire, P. G., and N. W. Seeds. 1989. The interaction of plasminogen activator with a reconstituted basement membrane matrix and extracellular macromolecules produced by cultured epithelial cells. *J. Cell. Biochem.* 40:215–227.

41. Guy-Grand, D., C. Griscelli, and P. Vassalli. 1978. The mouse gut T lymphocyte, a novel type of T cell: nature, origin, and traffic in mice in normal and graft-versus-host conditions. *J. Exp. Med.* 148:1661–1677.

42. Dobbins, W. O., III. 1986. Human intestinal intraepithelial lymphocytes. *Gut.* 27:972–985.

43. Kedinger, M., K. Haffen, and P. Simon-Assmann. 1987. Intestinal tissue and cell cultures. *Differentiation.* 36:71–85.

44. Hahn, U., D. Schuppan, E. G. Hahn, H.-J. Merker, and E.-O. Reicken. 1987. Intestinal cells produce basement membrane proteins in vitro. *Gut.* 28(Suppl. 1):143–151.

45. Simon-Assmann, P., K. Bouziges, C. Arnold, K. Haffen, and M. Kedinger. 1988. Epithelial-mesenchymal interactions in the production of basement membrane components in the gut. *Development (Camb.).* 102:339–347.

46. Simon-Assmann, P., F. Bouziges, M. Vigney, and M. Kedinger. 1989. Origin and deposition of basement membrane heparan sulfate proteoglycan in the developing intestine. *J. Cell Biol.* 109:1837–1848.

47. Senior, P. V., D. R. Critchley, F. Beck, R. A. Walker, and J. M. Varley. 1988. The localization of laminin mRNA and protein in the postimplantation embryo and placenta of the mouse: an in situ hybridization and immunocytochemical study. *Development (Camb.).* 104:431–446.

48. Weiser, M. M., D. Sikes, and P. Killen. 1989. Rat intestinal basement membrane synthesis and enterocyte differentiation. *Clin. Res.* 37:599A. (Abstr.)